Computational insight on CO_2 fixation to produce styrene carbonate assisted by a single centre Al(III) catalyst and quaternary ammonium salts

Valeria Butera,[a] Nino Russo,[b] Ugo Cosentino,[a] Claudio Greco,[a] Giorgio Moro,[c] Demetrio Pitea,[a] and Emilia Sicilia*[b]

Abstract: Density functional theory (DFT) was used to investigate the cycloaddition reaction of CO_2 to styrene oxide for the formation of styrene carbonate. The uncatalyzed process alongside the reactions assisted by tetrabutylammonium bromide (**TBAB**), the novel non-symmetrical single-centre aluminium(III) salen-acac hybrid complex (salenac) (**Al1cat**) and the binary **Al1cat/TBAB** system are all investigated and for all of them the optimized structures, rate-determining steps and lowest energy barrier reaction pathways have been intercepted for both gas-phase and solvent environments. The reaction, in absence of the catalyst, proceeds through nucleophilic attack from an oxygen atom of CO_2 on either the α carbon (most substituted carbon) or the β carbon (least substituted carbon) atom of styrene oxide, **SO**, by overcoming very high energy barriers. In the case of catalyzed systems, the reaction mechanism consists of three key elementary steps: 1) epoxy ring opening; 2) CO_2 electrophilic attack and 3) intramolecular cyclization. In presence of Al1cat, the central metal of the catalyst coordinates with an oxygen atom of epoxide, activating it towards a nucleophilic attack by the halide. An oxy anion species is formed, that affords the corresponding cyclic carbonate after reaction with CO_2. Our results provide important hints on the cycloaddition of CO_2 and epoxides promoted by non-symmetrical aluminium complex containing a single metal center, and can satisfactorily explain the previous experimental observations allowing the development of more efficient catalysts for organic carbonate production.

Introduction

Since petroleum resources are predicted to be exhausted at the current rate of consumption “in the next 70 years”, there is an ever-growing effort to develop new chemical processes using renewables. The use of carbon dioxide (CO_2) is drawing much interest because of its abundance, low cost, nontoxicity, and high potential as a renewable resource.[1] The highly versatile nature of CO_2 has been exploited in numerous industrial applications, although the thermodynamic stability of CO_2 has hampered its use as a reagent for chemical synthesis.[2,3] One of the most promising methodologies in the utilization of CO_2 is the synthesis of cyclic carbonates via cycloaddition of CO_2. Cyclic carbonates, that are generally produced using phosgene as a (toxic) reagent resulting in hazardous waste streams,[4] are valuable products widely used as green solvents, electrolytes, fuel additives and intermediates for polycarbonates. Furthermore, the formation of cyclic carbonates is an example of atom efficient reaction with each atom present in the two reactants being incorporated into the final product. However, due to the high thermodynamic stability and low reactivity of CO_2, catalysts are needed to reduce the activation energy of any kind of reaction in which it is implicated. In this context, significant efforts have been devoted to the development of efficient homogeneous catalytic systems, able to assist the synthesis of cyclic carbonates from epoxides by carbon dioxide cycloaddition, even if for many of them the catalytic activity is low and high temperatures/pressures are required. Many different catalytic solutions have been proposed as ionic liquids,[5] binary[6] or bifunctional complexes[7] and simple motifs as quaternary onium salts, such as ammonium salts, that have shown to exhibit high activity and stability for this reaction.[8] Very recently a combination of tetraalkyl-ammonium halides and cavitand hosts has been used to catalyze carboxylation of styrene oxide.[9] The mechanism of conversion of CO_2 and ethylene oxide into ethylene carbonate catalyzed by tetraethylammonium bromide, **Et_4NBr** has been elucidated only recently by Zhang and co-workers.[10] In that combined experimental and theoretical study, structural and energetic information concerning each step of the catalytic cycle are reported and the influence of the N-alkyl chain length and the type of anion on the outcomes is also evaluated. Among the very numerous metal complexes proposed for the cycloaddition reaction, a particular attention has been focused on the highly active (salen)metal-based catalytic systems such as manganese,[11] chromium,[12] cobalt,[13] and zinc[14] salen complexes. However, for some of these complexes high metal toxicity, especially cobalt and chromium, and difficulty to be completely separated from products limit the potential application in industry. In the effort to use more environmentally benign metal complexes, a considerable interest in the synthesis of cyclic carbonates has been devoted to homogeneous salen complexes of aluminium, which is also highly abundant on Earth and possesses a high catalytic activity under mild conditions.[15] There is much precedent in the literature for the employment of symmetrical (salen)aluminium complexes in presence of Lewis bases as cocatalyst, including quaternary ammonium salts,

[a] Dr. V. Butera, Prof. Dr. U. Cosentino, Dr. C. Greco, Prof. Dr. D. Pitea
Dipartimento di Scienze dell’Ambiente e del Territorio e di Scienze della Terra, Università degli Studi Milano-Bicocca Piazza della Scienza 1, 20126 Milano, Italy
[b] Prof. N. Russo, Prof. Dr. E. Sicilia
Dipartimento di Chimica e Tecnologie Chimiche,
Universita` della Calabria, 87036 Arcavacata di Rende (CS), Italy.
siciliae@unical.it
[c] Prof. Dr. G. Moro
Dipartimento di Biotecnologie e Bioscienze, Università degli Studi Milano-Bicocca Piazza della Scienza 2, 20126 Milano, Italy
Supporting information for this article is available on the WWW under http://dx.doi.org/

serving as binary catalysts for transforming CO_2/epoxides into cyclic carbonates.[16] A bimetallic complex Al(salen)−O−Al(salen), which showed to be an effective catalyst under ambient conditions for the reaction, was discussed by North et al.[6d] in 2009. Styring and coworkers reported, very recently, the synthesis of styrene carbonate using the novel non-symmetrical aluminium(III) salen-acac hybrid complex (salenac), labeled **Al1cat**,[17] that displayed a better catalytic activity than the symmetrical (salen)AlCl complex[15] at low CO_2 pressure. The authors also demonstrated that the presence of the quaternary ammonium salt, tetrabutylammonium bromide, **TBAB** (Scheme 1) enhances the catalytic activity and stability for this reaction, increasing the conversion from 70%, using the catalyst alone, to 90% when **TBAB** is added as a co-catalyst. **TBAB** alone, instead, was found to be as effective as **Al1cat** alone. Furthermore, an induc-tion period has been observed in the reaction catalyzed by both the **Al1cat** alone and the **Al1cat**/**TBAB** binary system. For both catalysts this period is reduced with increasing the temperature, whereas at the same temperature the binary system shows a shorter induction period than **Al1cat** alone.

Scheme 1. Cyclic styrene carbonate synthesis through CO_2 insertion into styrene oxide.

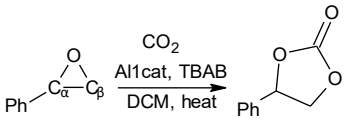

As it is extensively reported in the literature,[18] the binary catalytic system combining a Lewis acid and a suitable nucleophile (most often a halide) makes the ring-opening procedure less energetically demanding and the subsequent CO_2 insertion easier. The proposed mechanism for the **Al1cat**/**TBAB** catalyzed synthesis of cyclic carbonates from epoxides and carbon dioxide is reported in Scheme 2.

Scheme 2. Proposed mechanism for the **Al1cat/TBAB** catalyzed synthesis of cyclic carbonates from epoxides and carbon dioxide.

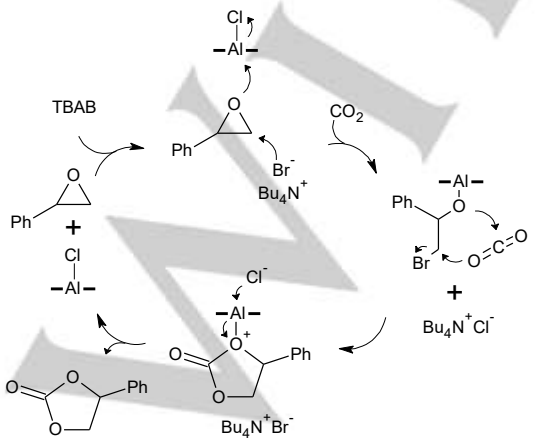

To develop a basic understanding of the interactions of CO_2 with activating species, calculations are of considerable importance for the investigation of transition states and barriers, thermodynamics and change in electronic structure and for spectroscopic simulations. Owing to such interest, several theoretical calculations[6g,10,18a,19] have been carried out giving insight into mechanistic details of the catalytic CO_2 activation in homogeneous phase, which would pave the way to the design of efficient, tailor-made molecular catalysts. In this context, we have undertaken a quantum-mechanical investigation of the fixation process of CO_2 with styrene oxide for the formation of a cyclic carbonate assisted by the non-symmetrical aluminum catalyst **Al1cat** in order to provide a molecular level understanding of the reaction process, which could allow the rational development of more powerful catalytic systems. The non-catalyzed reaction has been also studied at the same level of theory in order to evaluate, besides a comparison with analogous literature data, how the presence of the catalyst can reduce the energy barrier. The cycloaddition reaction catalyzed by the binary system **Al1cat**/**TBAB** has been also compared with that of **Al1cat** and **TBAB** alone to verify the effective improving of the catalytic activity in presence of the binary catalyst.

Results and Discussion

In the following sections we illustrate the outcomes of our computational analysis of the uncatalyzed and catalyzed addition reaction of CO_2 to styrene oxide, both in vacuo and in solution. Results in gas-phase will be analyzed only for the aim of comparison with analogous previously reported results that do not include solvent effects.

Uncatalyzed cycloaddition reaction of CO_2

The uncatalyzed cycloaddition reaction of CO_2 to styrene oxide **SO** leads to the formation of styrene carbonate, **SC**, through only one elementary step. Two possible reaction pathways of CO_2 cycloaddition have to be taken into account and the energy profiles describing the intercepted minima and transition states are illustrated in Figure 1. The values of the most relevant geometrical parameters can be found in the Supporting Information (SI) (Figure S1). The former pathway corresponds to the nucleophilic attack from an oxygen atom of CO_2 on the α carbon (most substituted carbon) of the styrene epoxide. The latter considers the same nucleophilic attack on the β carbon (least substituted carbon) of **SO**. Our computed results show that the formation of the **SC** product, that lies at 27.1 kcal·mol^{-1} below the entrance channel of the reaction, is a highly exothermic process. This is in agreement with the experimental findings that give a value of ΔH_r= -33.5 kcal·mol^{-1}.[20] The unique imaginary vibrational frequency, 285.9*i* cm^{-1}, of $\mathbf{TS_\alpha}$ corresponds to the contemporary breaking of the C_α-O bond of the epoxide and the simultaneous formation of two new C-O bonds, originating from the insertion of CO_2, with the consequent formation of the cyclic carbonate product. In an analogous manner, through the $\mathbf{TS_\beta}$ (689.1*i* cm^{-1}), the breaking of the C_β-O bond and the insertion of

CO_2 the same final product is produced. The calculated free energy barriers are very high and correspond to 44.1 kcal·mol^{-1} for the α pathway and 49.1 kcal·mol^{-1} for the β pathway. Therefore, we find that the α pathway is favored by 5.0 kcal·mol^{-1} with respect to the β pathway. The stabilization of the positive charge on C_α atom by the resonance effect of the aromatic ring makes the TS_α more stable. This difference becomes even higher (about 15 kcal·mol^{-1}) when the zero-point corrected energies are examined. In this case, the values of the relative energy barriers are 45.7 and 60.8 kcal·mol^{-1} for the α and β pathways respectively. Zhang and co-workers obtained an energy-barrier of 53.4 kcal·mol^{-1} for the α pathway and 58.1 kcal·mol^{-1} for the β pathway examining CO_2 coupling with ethylene oxide.[19g] Han and co-workers reported energy barriers of 55.3 and 61.4 kcal·mol^{-1} for the α and β pathways, respectively for the reaction with propylene oxide.[19a] A free energy barrier of 66.2 kcal·mol^{-1} is reported in ref. 19b for the attack on the β carbon. All these results confirm that catalysts have to be introduced to

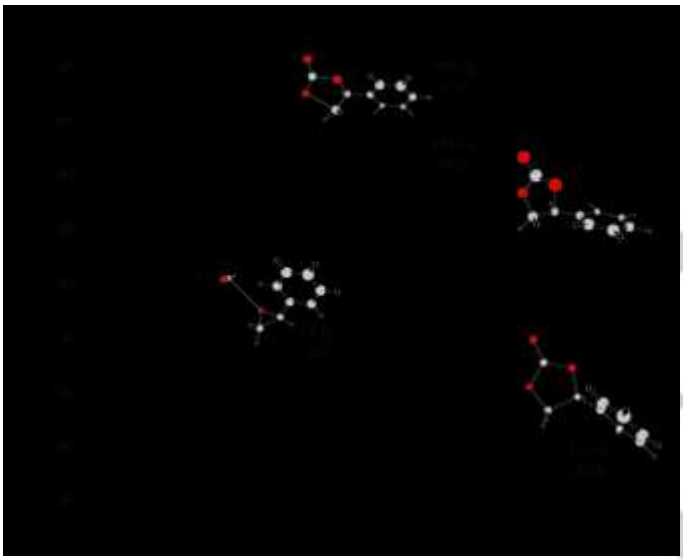

Figure 1. B3LYP free energy profiles for the uncatalyzed attack of CO_2 on the α carbon (dashed line) and β carbon (solid line) of styrene oxide, **SO**, to give styrene carbonate, **SC**. Gas-phase, zero-point-corrected energy changes are reported in parentheses. Energies are in kcal·mol^{-1} and relative to reactants' asymptote.

reduce the non-catalyzed cycloaddition reaction energy barriers, calculated to be too high for the reaction to occur spontaneously. The high exothermicity of the process[20] is also well reproduced by our results.

Cycloaddition reaction of CO_2 catalyzed by quaternary ammonium salts

A detailed DFT investigation for the elucidation of the mechanism of conversion of styrene oxide with CO_2 catalyzed by tetrabuthylammonium bromide, **TBAB**, has been carried out according to the mechanistic scheme for fixation of CO_2 with epoxides catalyzed by quaternary ammonium salts proposed by Calò and co-workers[8a] and Styring et al., [17] who have found, as mentioned above, that the catalytic activity of **TBAB** alone is comparable to that of **Al1cat** system. The authors suggest that the nucleophilic attack by the bromide ion is responsible of the epoxide ring opening with the consequent formation of an oxy anion species. Reaction with CO_2 leads to the formation of the corresponding cyclic carbonate. In order to reduce the computational effort, our computational analysis of the energy profiles has been carried out by using instead of **TBAB** the simplified catalyst model tetramethylammonium bromide, **TMAB**. Support to this choice comes from the previous research by Zhang and co-workers,[10] whose DFT investigation demonstrated that both chain length and identity of the anion of quaternary ammonium salts have little influence on the yields and conversion of the epoxides when the same substrate is involved. The proposed reaction mechanism consists of three elementary steps as shown in Fig. 2. More information on the geometrical structures of stationary points intercepted along the energy profiles is reported in the SI (Figure S2).

Initially, **SO** and **TMAB** interact to form a complex $\mathbf{1_{TMAB}}$ from which, in analogy with the uncatalyzed reaction mechanism, we can distinguish two different α and β pathways. Along α pathway, through $\mathbf{TS1_{\alpha TMAB}}$, $\mathbf{1_{TMAB}}$ complex could be converted into intermediate $\mathbf{2_{\alpha TMAB}}$ by over-coming a barrier of 22.3 kcal·mol^{-1}. Along the β pathway, formation of the $\mathbf{2_{\beta TMAB}}$ intermediate takes place, that lies 10.1 kcal·mol^{-1} above the reactants' dissociation limit and the height of the barrier for the transition state leading to it is 22.9 kcal·mol^{-1}. The calculated energy barriers for this first step, that represents the rate determining step for both the α and β pathways, are very similar. When the zero-point corrected energies in gas-phase are considered, higher energy barriers of 27.7 kcal·mol^{-1} for the α and 29.4 kcal·mol^{-1} for the β pathways are found. These values are similar to that of 29.8 kcal mol^{-1} computed by Zhang and co-workers for the analogous step of the reaction between **Et$_4$NBr** and ethylene oxide.[10] After the addition of CO_2 into the reaction system, the new complexes $\mathbf{3_{\alpha TMAB}}$ and $\mathbf{3_{\beta TMAB}}$ are directly formed, being the complex $\mathbf{3_{\alpha TMAB}}$ calculated to be slightly more stable with respect to $\mathbf{3_{\beta TMAB}}$. The next step leads to formation, along both α and β pathways, of the cyclic carbonate product via the transition states $\mathbf{TS2_{\alpha TMAB}}$ and $\mathbf{TS2_{\alpha TMAB}}$, corresponding to the concerted ring closure and release of the bromide anion.

Such transition states lie 9.3 and 6.5 kcal·mol^{-1} below the reference energy and the corresponding computed barriers are 9.1 and 11.3 kcal·mol^{-1}, respectively. Considering the gas-phase energy barriers, a good agreement of our computed value for the α favored route, 16.9 kcal·mol^{-1}, and that reported in literature for the ethylene oxide, 18.0 kcal·mol^{-1}, is found[10]. The release of the restored **TMAB** catalyst requires 10.9 kcal·mol^{-1} to occur.

In comparison with the uncatalyzed reaction, the energy barrier for the **TMAB**-catalyzed cycloaddition is reduced by 21.8 kcal·mol^{-1} when the α pathway is considered and 26.2 kcal·mol^{-1} for the β one. Our results show that the calculated stability of minima and heights of the barriers make the α path the slightly preferred one, even if both pathways become accessible with increasing the temperature. Estimation is given of the advantageous lowering of the energy barrier when the reaction is assisted by a quaternary onium salt catalyst.

Figure 2. Free energy surface alongside optimized structures of minima and transition states for the **TMAB**-catalyzed fixation of CO_2 with styrene oxide. The attack on both the C_α (solid line) and C_β (dashed line) carbon of epoxide are reported. Gas-phase, zero-point-corrected energy changes are reported in parentheses. Energies are in kcal·mol^{-1} and relative to reactants' asymptote.

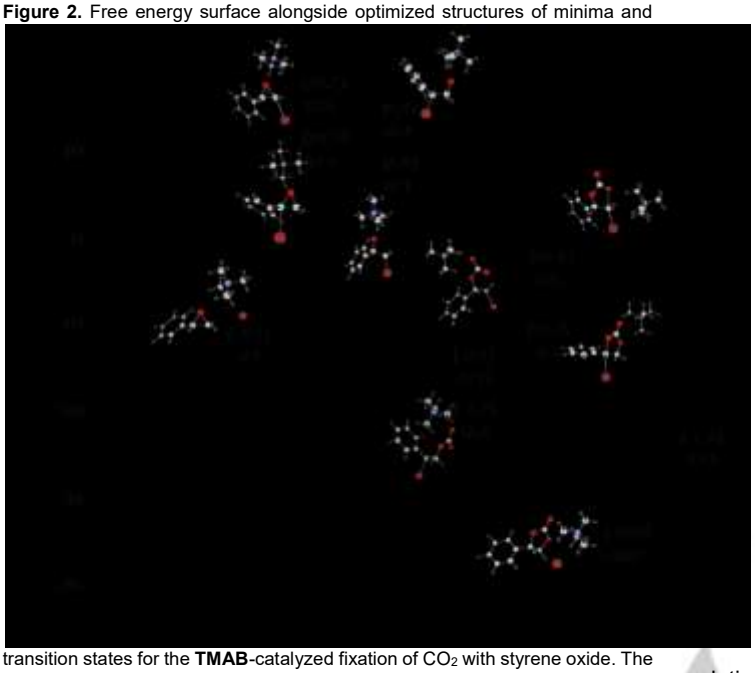

Al1cat catalyzed cycloaddition reaction

Similarly to the uncatalyzed and **TMAB**-catalyzed reaction, the cycloaddition reaction of CO_2 to styrene oxide catalyzed by **Al1cat** complex can involve two possible reaction pathways. In Figure 3 and 4 are shown the α free energy profile and the optimized structures of the intercepted intermediates and transitions states, respectively. All the details concerning the β free energy profile are available in the SI (Figure S3 and S4). The sum of the isolated reactants energies, **Al1cat**, CO_2 and **SO**, is set as zero for the calculation of relative energies. For both the α and β routes, the reaction starts with the formation of a minimum, labeled **Int1**$_{\mathbf{Al1cat}}$, in which the epoxide is close to the **Al1cat**. Such adduct lies 3.4 kcal·mol^{-1} below the reference energy of separated reactants. The reaction proceeds with the coordination of the epoxide to the metal center and the consequent release of the chloride anion via the **TS1-2**$_{\mathbf{Al1cat}}$ by overcoming an energy barrier of 33.9 kcal·mol^{-1} that leads to the formation of the **Int2**$_{\mathbf{Al1cat}}$. This common step is found to be the rate determining step for both the studied mechanisms.

Epoxide coordination to the Al polarizes the C-O epoxide bonds thereby facilitating the ring-opening step that can occur following the two α and β alternative pathways. The NBO charge analysis shows that in going from **Int1**$_{\mathbf{Al1cat}}$ to **Int2**$_{\mathbf{Al1cat}}$ the charge on the C_α carbon becomes more positive and that on C_β less negative (see Supporting Information) and the α pathway is calculated to be kinetically more accessible. Following the α path, reported in Figure 3, the nucleophilic chloride attacks the more substituted C_α atom of the coordinated epoxide, through **TS2-3α**$_{\mathbf{Al1cat}}$ and causes the breaking of the C_α-O bond of the epoxide and the simultaneous formation of the new C_α-Cl bond as confirmed by a unique imaginary frequency of 303*i* cm^{-1}. The **Int3α**$_{\mathbf{Al1cat}}$ intermediate is formed by surmounting a lower energy barrier than the analogous barrier along the β path (3.4 kcal·mol^{-1} versus 6.4 kcal·mol^{-1}). This difference in the height of the energy barriers at the bifurcation between α and β paths makes the attack at the α carbon more accessible than that at the β carbon. NBO charge analysis reveals a more pronounced electrophilic character of C_α carbon with respect to C_β that justifies this difference. Intermediates **Int3α**$_{\mathbf{Al1cat}}$ and **Int3β**$_{\mathbf{Al1cat}}$ lye at 26.0 and 26.3 kcal·mol^{-1}, respectively below the reference energy. When CO_2 enters into the reaction system, the new complexes **Int4α**$_{\mathbf{Al1cat}}$ and **Int4β**$_{\mathbf{Al1cat}}$ are formed. Such intermediates are less stable by 9.2 kcal·mol^{-1} and 7.6 kcal·mol^{-1} respectively than the relative previous intermediates mainly due to the entropic cost for bringing together **Int3** and CO_2. Following both α and β paths, in the subsequent step, the CO_2 insertion occurs by reaction with the negatively charged oxygen atom of the intermediates **Int4α/β**$_{\mathbf{Al1cat}}$, leading to the formation of linear carbonates, labeled **Int5α**$_{\mathbf{Al1cat}}$ and **Int5β**$_{\mathbf{Al1cat}}$ through the corresponding transition states **TS4-5α/β**$_{\mathbf{Al1cat}}$. In this case, the imaginary frequencies at 196.8*i* cm^{-1} for α pathway and 150.7*i* cm^{-1} for the

Figure 3. Free energy profile for the **Al1cat** catalyzed fixation of CO_2 with styrene oxide. The attack on the C_α carbon of epoxide is reported. Gas-phase, zero-point-corrected energy changes are reported in parentheses. Energies are in kcal·mol^{-1} and relative to reactants' asymptote.

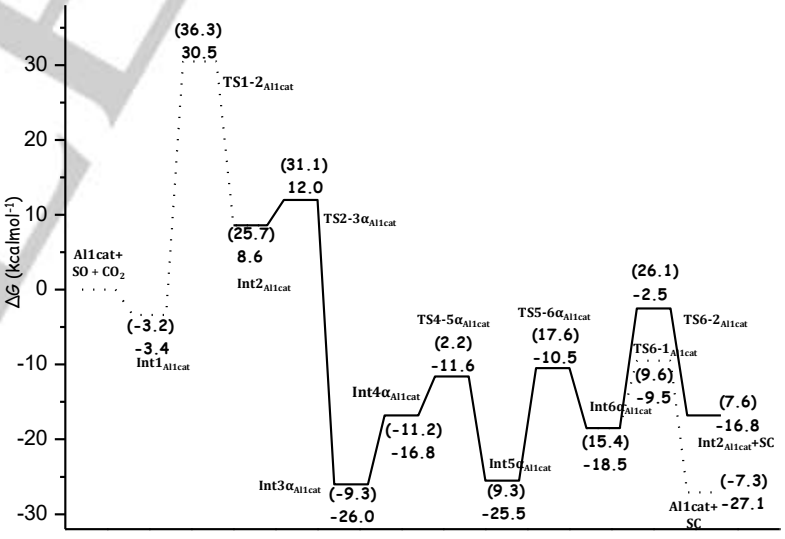

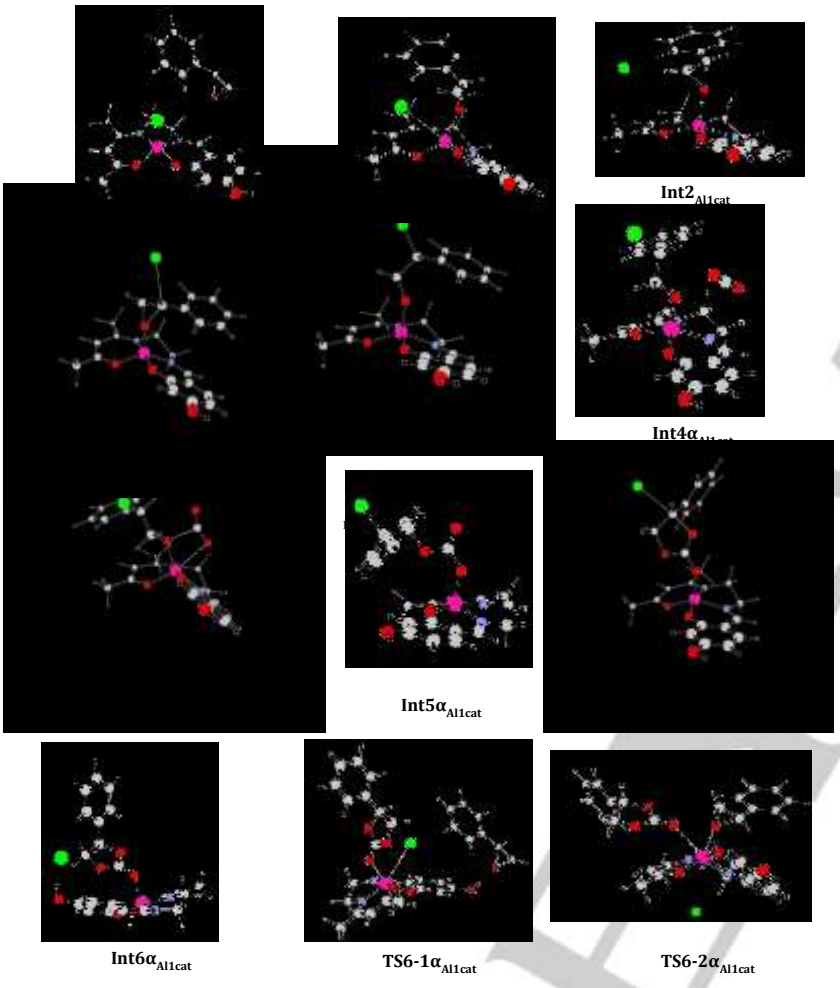

Figure 4. Optimized structures of minima and transition states intercepted along the **Al1cat** catalyzed fixation of CO_2 with styrene oxide for the attack on the C_α carbon of epoxide. Bond distances are in Å

β route are associated to the formation of new C-O and Al-O bonds between the chloro-alkoxide species and CO2 molecule. The two calculated very similar energy barriers along the α and β routes are 5.2 and 6.2 kcal·mol^{-1}, respectively. linear carbonate intermediates **Int5α/β$_{Al1cat}$** undergo an intramolecular ring-closing with the concomitant release of the chloride nucleophile and formation of the **SC** final product. In this latter step, the carbon atom bound to the chloride forms a new bond with the nearest oxygen atom and, simultaneously, the chloride bond elongates until it breaks (Figures 3 and 4). The ring-closing

step costs 15.0 kcal mol^{-1} along the α pathway, that is 2.5 kcal·mol^{-1} higher than the β pathway. Once the cyclic carbonate is formed, the reaction, as it is illustrated in Figure 3, can proceed allowing further epoxide turnover either restoring the **Al1cat** complex due to reattachment at the Al center of the displaced chloride anion(**TS6-1$_{Al1cat}$** and dashed line in Figure 3) or by coordination of a new **SO** molecule in place of the formed **SC** (**TS6-2$_{Al1cat}$** and solid line in Figure 3). In the former case the activation barrier is 9.0 kcal mol^{-1}. The catalytic cycle can restart with the coordination of the epoxide to the metal center of the regenerated **Al1cat** catalyst and the ensuing release of the chloride anion, which represents the rate determining step of the overall mechanism. In the latter case, by overcoming an energy barrier of 16.0 kcal·mol^{-1} the **Int2$_{Al1cat}$** intermediate together with the released **SC** product are directly formed avoiding the very high energy barrier involved in the first step. Such barrier can be considered responsible of the observed induction period and the **Al1cat** some sort of pre-catalyst that makes available the Cl^- nucleophile. If the high barrier relative to the first step is included the height of the barrier of the slowest step undergoes a reduction of 10.2 kcal·mol^{-1} in comparison with the corresponding uncatalyzed α process, caused by a **Al1cat** induced polarization of the substrate C-O bond that facilitates CO_2 activation. The energetic cost is significantly reduced in the next catalytic cycles if we assume that they start directly from the **Int2$_{Al1cat}$** complex. Once this hypothesis is accepted, our results agree well with experimental results that found **TBAB** alone catalytic activity comparable to that of **Al1cat** alone. The overall computational description of the process given here is able to rationalize the information coming from experiments[17] even though the experimentally estimated height of 8.1 kcal·mol^{-1} of the energy barrier is considerably lower than any of the values calculated here.

Al1cat/TBAB catalyzed cycloaddition reaction

As reported above, in presence of **Al1cat** alone, the reaction mechanism involves firstly the coordination of the oxygen atom of the epoxide to the metal center that results in a cleavage of the Al-Cl bond. Once the chloride anion is released, the ring-opening occurs in a second step through nucleophilic attack of the chloride on C_α or C_β atoms of the epoxide. The proposed mechanism for the binary system **Al1cat**/**TMAB** is remarkably similar to that assisted by the **Al1cat** catalyst. However, when the binary system is considered, the nucleophilic bromide can directly attack the epoxide, activated by the aluminum catalyst, leading to the opening of the epoxide ring and the release of the chloride. This concerted mechanism in the case of the binary catalyst should have lower activation energy than in the metal-free system, where the bromide nucleophilic attack at the epoxide occurs without prior activation. DFT analysis was performed to computationally examine the effect of the combined Al1cat and TBAB catalytic system. The assistance of the ammonium salt was simulated by including only the bromine anion. Again two different catalytic pathways, α and β attacks on

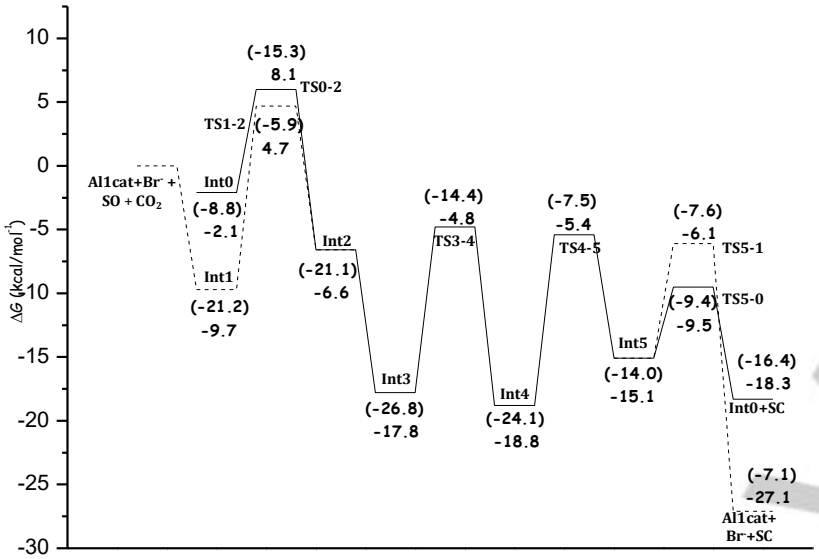

Figure 5. Free energy surface for the **Al1cat/TBAB** catalyzed fixation of CO_2 with styrene oxide. The attack on the C_α carbon of epoxide is reported. Gas-phase, zero-point-corrected energy changes are reported in parentheses. Energies are in kcal·mol^{-1} and relative to reactants' asymptote

the epoxide, have been described in analogy with the uncatalyzed TMAB- and Al1cat-catalyzed cycloaddition reaction. Figure 5 shows the free energy profiles and Figure 6 the optimized structures of the minima and transition states that are involved in the binary **Al1cat/TBAB** catalyzed CO_2 activation reaction, considering the α pathway. Energy profile and stationary point geometrical structures for the attack on the Cβ carbon are available in the SI (Figures S5 and S6). When the binary system is taken into account, the first step of the catalytic cycle is the energetically favorable formation of a first adduct, **Int1** in Figures 5 and 6, thanks to the interaction between the catalyst, the epoxide and the bromide anion of the salt. The formation of **Int1**, which lies at 9.7 kcal·mol^{-1} below the reactants' asymptote, is the first common step for both the α and β pathways.

The highly reactive anion of the **TBAB** quaternary ammonium salt catalyzes the opening of the epoxide ring by nucleophilic attack. When the halide attacks the most substituted carbon atom of the epoxide, the **Int2** intermediate is formed through **TS1-2**, with an energy barrier of 14.4 kcal·mol^{-1}. In an analogous manner seen for the **Al1cat**, the addition of the CO_2 molecule leads to the formation of the intermediate **Int3**. This adduct is more stable with respect to the previous intermediate by 11.2 kcal·mol^{-1}. This energy stabilization is caused by strong electrostatic interactions that the negatively charged chloride anion establishes with the aluminium ligand alongside the interaction between the negatively charged oxygen atom of the epoxide and the partly positive carbon of the CO_2 molecule. The **Int4** bromo-alkoxide specie is afforded through the transition state **TS3-4** by surmounting an energy barrier of 13.0 kcal·mol^{-1}. The formed **Int4** undergoes an intramolecular ring-closure with the concomitant release of the bromide nucleophile and formation of the **SC** product. The energy required to overcome the corresponding barrier is 13.3 kcal·mol^{-1}. In analogy with the mechanism described in presence of **Al1cat** alone**,** once the coordinated cyclic carbonate is formed, further epoxide turnover is accomplished by either **Al1cat** complex regeneration due to displacement of the **SC** product and re-coordination of the chloride or release of the product thanks to the coordination of the epoxide. Re-coordination of the chloride costs 9.0 kcal·mol^{-1} (**TS5-1** and dashed line in Figure 5) and leads to the regeneration of the **Al1cat** that is ready to undergone a new **SO** attack. Displacement of the formed **SC** by a new **SO** molecule, instead, requires 5.6 kcal·mol^{-1} to occur (**TS5-0** and solid line in Figure 5). In this latter case a new intermediate is formed, labeled **Int0**, together with the released **SC** product. At the entrance channel **Int0** is calculated to be stabilized by 2.1 kcal·mol^{-1} and when is attacked by the bromide anion, leads to the formation, once again, of the **Int2** intermediate, via the transition state **TS5-0**. Such transition state lies 8.1 kcal·mol^{-1} above the reference energy of separated reactants and, consequently, the energy barrier that is necessary to overcome is 8.8 kcal·mol^{-1}. Since the barrier for the first step at the first cycle is 14.4 kcal·mol^{-1} this might be the reason why for the binary catalyst as well as the **Al1cat**, an induction period is observed. Moreover, due to the different heights of the bypassed barriers (14.4 kcal·mol^{-1} versus 33.9 kcal·mol^{-1}), the shorter induction period detected for the binary system can be rationalized.

Along the β path, after the formation of the **Int1** adduct, **Int2'** can be produced by a less favoured mechanism that proceeds by a nucleophilic attack of the bromide anion on the C_β. The energy barrier associated to this step is 18.6 kcal·mol^{-1}, that is 4.2 kcal·mol^{-1} higher with respect to the α route. The transition state is characterized by the cleavage of the C_β-O bond and the formation of Al-O and C_β-Br bonds. The second transition state **TS'3-4** leads to the formation of new O-C and Al-O bonds by activation of the CO_2 molecule and the contemporaneous breaking of the bond between the metal center and the epoxide oxygen.

The rate determining step along the β pathway is the formation of the cyclic carbonate with an energy barrier of 19.4 kcal·mol^{-1} that is higher than that of 14.4 kcal·mol^{-1} calculated for the α path rate-determining step. In comparison with analogous calculations performed by Kleij and coworkers,[6g] to computationally describe, adopting the B3LYP functional and including solvent effects, the CO_2 addition to propylene oxide catalyzed by an Al(III) amino-tris(phenolate) complex and NBu_4I as co-catalyst the energetics of intercepted minima for the first ring opening step is very similar, whereas the barrier for the first

transition state is higher. Furthermore, CO_2 insertion step has been calculated to be rate-limiting.

Also in the case of the binary system, the α path appears to be favoured with respect to the β one. The results reported here are in a satisfactory agreement with reported experimental evidences.[17] Nevertheless, as in the case of **Al1cat** alone, the barrier of 5.5 kcal·mol^{-1} estimated by the Arrhenius plot is very low with respect to calculated barriers whatever kind of mechanism and pathway is taken into consideration.

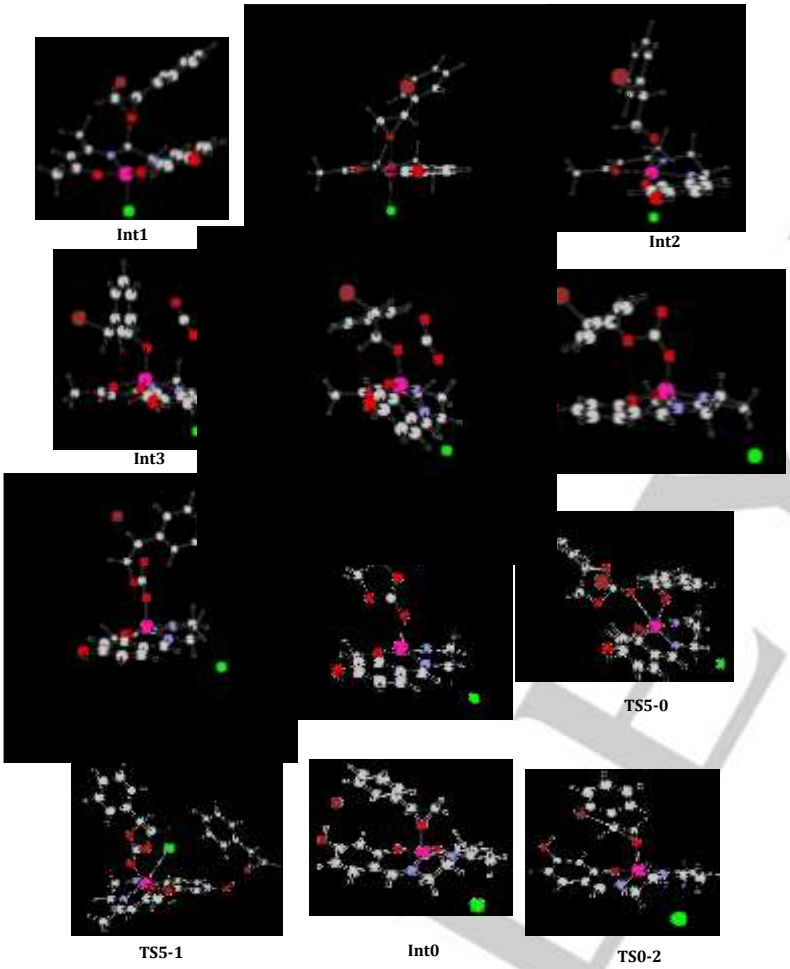

Figure 6. Optimized structures of stationary points for the **Al1cat/TBAB** catalyzed fixation of CO_2 with styrene oxide. The attack on the C_α carbon of epoxide is reported. Gas-phase, zero-point-corrected energy changes are reported in parentheses. Energies are in kcal·mol^{-1} and relative to reactants' asymptote.

Conclusions

A rigorous quantum-mechanical investigation of the mechanism for the cycloaddition of CO_2 to epoxides, namely styrene oxide, catalyzed by the binary **Al1cat/TMAB** catalyst system was performed. The outcomes of the computational analysis carried out here confirm the experimental findings furnishing the explanation of why the cycloaddition of CO_2 to styrene oxide proceeds in an easier way in presence of the binary **Al1cat/TBAB** catalyst compared with both the non-catalyzed and the **TBAB**- and **Al1cat**-catalyzed routes. For all the studied systems, the cycloaddition reaction of CO_2 to the epoxide can involve two possible reaction pathways: the nucleophilic attack can occur on both the α carbon (most substituted carbon) and the β carbon (least substituted carbon) atom of styrene epoxide. The α path is slightly favored in comparison with the β route for all the studied mechanisms. In absence of any catalyst, the nucleophile is an oxygen atom of CO_2 and the formation of the cyclic carbonate occurs through only one elementary step. As expected, high energy-barriers of 44.1 kcal·mol^{-1} for the α pathway and 49.1 kcal·mol^{-1} for the β one are calculated. When the **TBAB** catalyst, modeled by the simplified model catalyst **TMAB** to reduce the computational effort, is added to the reaction system, the rate-determining step activation energy becomes 22.3 kcal·mol^{-1} along the α path and corresponds to the opening of the epoxide due a nucleophilic attack by the bromide ion. The formed oxy anion species reacts with CO_2 leading to the formation of the corresponding cyclic carbonate. The presence of **Al1cat** entails the epoxide coordination to the Al atom with the consequent polarization of the C-O epoxide bond, that facilitates the ring-opening step. However, when only **Al1cat** is present, the first step of the catalytic cycle, that is also the rate-determining step ($\Delta G^{\#}$ = 33.9 kcal·mol^{-1}), is the replacement of the chloride anion by the epoxide ring. The released chloride, in the next step, attacks either the C_α or the C_β atom of the styrene oxide forming the corresponding linear chloro-alkoxide specie coordinated to the metal center, that reacts with the carbon dioxide molecule in order to form the styrene carbonate via an intramolecular cyclisation reaction. In presence of **TMAB** as co-catalyst, the highly reactive anion of the quaternary ammonium salt can directly attack the epoxide leading to the opening of styrene oxide and the contemporaneous release of the chloride anion. The calculated free energy barrier of such step, that also represents the rate determining step, is only 14.4 kcal·mol^{-1}. The consequent step implies the CO_2 insertion reaction (13.0 kcal·mol^{-1}). The induction period experimentally observed in the reaction catalyzed by both the **Al1cat** alone and the **Al1cat/TBAB** binary system can be rationalized when the possibility is taken into account that the last step of the catalytic cycle could be the coordination of a new **SO** molecule instead of the reattachment of the chloride to regenerate the **Al1cat**. Once this hypothesis is accepted our computational analysis confirms the experimental findings that the reaction proceeds as well with the organo-catalyst **TBAB** alone as it does with the aluminium catalyst alone**.** The computed slowest step barrier heights for both **Al1cat** and **Al1cat/TBAB** catalyzed reactions are, instead, higher than those experimentally estimated. Adequate rationalization of previous experimental observations furnished here should allow the development of

more efficient catalysts for organic carbonate formation using CO_2 as reactant.

Computational Details

All molecular geometries have been optimized at the Becke3-LYP (B3LYP) level of density functional theory.[21,22] Preliminary calculations have been carried out employing several exchange-correlation functionals, including functionals developed to properly take into consideration weak interactions, to test the reliability of the B3LYP results. Such calculations have demonstrated that the energetics is not significantly influenced by the inclusion of dispersion corrections. Moreover, benchmark calculations of the exothermicity of the whole process have shown as the chosen B3LYP functional is able to reproduce the experimental value of such quantity.[20]

Frequency calculations at the same level of theory have been also performed to identify all stationary points as minima (zero imaginary frequencies) or transition states (one imaginary frequency). The transition states involved have been checked by IRC (intrinsic reaction coordinate) analysis.[23,24] Standard 6-31G** basis sets of Pople and coworkers have been used for all atoms. Final energies have been calculated by performing single-point calculations on the optimized geometries at the same level of theory and employing 6-311+G(3dp,3df) standard basis sets. All the calculations have been carried out employing the Gaussian09 software package.[25] The impact of solvation effects on the energy profiles has been estimated by using the Tomasi's implicit Polarizable Continuum Model (PCM)[26] as implemented in Gaussian09. The UFF set of radii has been used to build-up the cavity. Since preliminary calculations clearly have shown that geometry relaxation effects are not significant, the solvation Gibbs free energies have been calculated in implicit dichloromethane (DCM ε=8.93), the solvent of experiments, at the same level performing single-point calculations on all stationary points structures obtained from vacuum calculations. Enthalpies and Gibbs free energies were obtained at 298 K at 1 atm from total energies, including zero-point, thermal and solvent corrections, using standard statistical procedures.[27] However, such approach does not reflect the real entropic change that occurs when the solute goes from the gas- to the condensed-phase, and the effects are more relevant when association and dissociation are involved. Therefore, following the procedure proposed by Wertz[28] to properly handle the change of translational and rotational entropy occurring when a solute is transferred from the gas phase into the solution phase, Gibbs free energies in solution for each species, have been calculated as:

$$G_{298K} = E_{elec} + G_{solv} + ZPE + H_{vib} + 6\,kT - T(S_{vib}) - T[0.54\times(S_{rot} + S_{trans} - 14.3) + 8.0],$$

where T= 298 K and the term 6 kT accounts for the potential and kinetic energies of the translational and rotational modes. More details can be found in the Supporting Information. NBO charge analysis has been carried out on the structures of some intercepted stationary points.[29]

Acknowledgements

This work has been financially supported by Universita` della Calabria and carried out within the FP7- PEOPLE-2011-IRSES, Project no. 295172.

Keywords: CO_2 fixation • styrene carbonate • DFT • Al(III) catalyst• homogeneous catalyst

[1] (a) W. L.Dai, S. F. Yin, C. T. Au, *Appl. Catal. A* **2009**, *366*, 2-12. (b) T. Sakakura, K. Kohno, *Chem. Commun*. **2009**, 1312-1330;

[2] (a) H. Arakawa, M. Aresta, J. N. Armour, M. A. Barteau, E. J. Beckman, A. T. Bell, J. E. Bercaw, C. Creutz, E. Dinjus, D. A. Dixon, K. Domen, D. L. DuBois, C. A. Eckert, E. Fujita, D. H. Gibson, W. A. Goddard, D. W. Goodman, J Keller, G. J. Kubas, H. H. Kung, J. E. Lyons, L. E. Manzer, T. J. Marks, K. Morokuma, K. M. Nicholas, R. Periana, L. Que, J. Rostrup-Nielson, W. M. H. Sachtler, L. D. Schmidt, A. Sen, G. A. Somorjai, P. C. Stair, B. R. Stults, W. Tumas, *Chem. Rev.* **2001**, *101*, 953–996; (b) T. Sakakura, J.-C. Choi, H. Yasuda, *Chem. Rev.* **2007**, *107*, 2365–2387.

[3] M. Aresta "Carbon Dioxide as Chemical Feedstock", *Wiley-VCH, Weinheim*, **2010**.

[4] R. Martín, A. W. Kleij, *ChemSusChem* **2011**, *4*, 1259-1263.

[5] (a) J. Sun, S.-I. Fujita, M. Arai, *J. Organomet. Chem.* **2005**, *690*, 3490–3497; (b) Y. Zhao, C. Yao, G. Chen, Q. Yuan, *Green Chem.* **2013**, *15*, 446–452; (c) Z.-Z. Yang, L.-N. He, C.-X. Miao, S. Chanfreau, *Adv. Synth. Catal.* **2010**, *352*, 2233–2240; (d) A.-L. Girard, N. Simon, M. Zanatta, S. Marmitt, P. Gonçalves, J. Dupont, *Green Chem*. **2014**, *16,* 2815–2825.

[6] (a) R. L. Paddock, S. T. Nguyen, *Chem. Commun.* **2004**, 1622; (b) C. Whiteoak, E. Martin, M. Martínez Belmonte, J. Benet-Buchholz, A. W. Kleij, *Adv. Synth. Catal.* **2012**, *354*, 469–476; (c) R. M. Haak, A. Decortes, E. C. Escudero-Adán, M. Martínez Belmonte, E. Martin, J. Benet-Buchholz, A. W.Kleij, *Inorg. Chem.* **2011**, *50*, 7934 –7936; (d) M. North, R. Pasquale, *Angew. Chem.* **2009**, *121*, 2990–2992; *Angew. Chem. Int. Ed.* **2009**, *48*, 2946–2948; (e) A. Decortes, M. Martínez Belmonte, J. Benet-Buchholz, A. W. Kleij, *Chem. Commun*. **2010**, *46*, 4580–4582; (f) J. Langanke, L. Greiner, W. Leitner, *Green Chem.* **2013**, *15*, 1173– 1182; (g) C. J. Whiteoak, N. Kielland, V. Laserna, F. Castro-Gomez, E. Martin, E. C. Escudero-Adán, C. Bo, A. W. Kleij, *Chem. Eur. J.* **2014**, *20,* 2264–2275.

[7] (a) A. Buchard, M. R. Kember, K. G. Sandeman, C. K. Williams, *Chem. Commun.* **2011**, *47*, 212–214; (b) T. Ema, Y. Miyazaki, S. Koyama, Y. Yano, T. Sakai, *Chem. Commun.* **2012**, 48, 4489–4491; (c) M. V. Escárcega-Bobadilla, M. Martínez Belmonte, E. Martin, E. C. Escudero-Adán, A. W. Kleij, *Chem. Eur. J.* **2013**, *19*, 2641–2648; (d) J. Melndez, M. North, P. Villuendas, C. Young, *Dalton Trans.* **2011**, *40*, 3885 –3902; (e) M. A. Fuchs, T. A. Zevaco, E. Ember, O. Walter, I. Held, E. Dinjus, M. Döring, *Dalton Trans*. **2013**, *42*, 5322–5329.

[8] (a) V. Calò, A. Nacci, A. Monopoli, A. Fanizzi, *Org. Lett.* **2002**, *4*, 2561–2563; (b) C.A. Montoyaa, A.B. Paninhoa, P.M. Felixa, M.E. Zakrzewskaa, J. Vitala, V. Najdanovic-Visakb, A.V.M. Nunes, *J. Supercrit. Fluids*, **2015**, *100*, 155–159.

[9] A. Mirabaud, J.-C. Mulatier, A. Martinez, J.-P. Dutasta, V. Dufaud, *ACS Catal.* **2015**, *5*, 6748−6752.

[10] J. Q. Wang, K. Dong, W. G. Cheng, J. Sun, S. J. Zhang, *Catal. Sci. Technol.* **2012**, *2*, 1480–1484.

[11] Y.Xiao, Z. Wang, K. Ding, *Macromolecules* **2006**, *39*, 128−137.

[12] (a) D. J. Darensbourg, J. C. Yarbrough, C. Ortiz, C. C. Fang, *J. Am. Chem. Soc.* **2003**, *125*, 7586−7591; (b) B. Li,; G. P. Wu,; W. M. Ren, Y. M. Wang, D. Y. Rao, X. B. Lu, *Polym. Chem.* **2008**, *46*, 6102−6113; (c) K. Nakano, M. Nakamura, K. Nozaki, *Macromolecules* **2009**, *42*, 6972−6980; (d) R. L. Paddock, S. T. Nguyen, *J. Am. Chem. Soc.* **2001**, *123*, 11498–11499.

[13] (a) Z. Qin, C. M. Thomas, S. Lee, G. W. Coates, *Angew. Chem., Int. Ed.* **2003**, *42*, 5484−5487; (b) G. P. Wu, S. H. Wei, W. M. Ren, X. B. Lu, T. Q. Xu, D. J. Darensbourg, *J. Am. Chem. Soc.* **2011**, *133*, 15191−15199; (c) E. K. Noh, S. J., S, S. Na, S. W. Kim, B. Y. Lee, *J. Am. Chem. Soc*. **2007**, *129*, 8082-8083; (d) S. Sujith, J. K. Min, J. E. Seong, S. J. Na, B. Y. Lee, *Angew. Chem., Int. Ed.* **2008**, *47*, 7306−7309; (e) W.-M. Ren, Z.-W. Liu, Y.-Q. Wen, R. Zhang, X.-B. Lu, *J. Am. Chem. Soc.* **2009**, *131*, 11509−11518.

[14] M. Cheng, D. R. Moore, J. J. Reczek, B. M. Chamberlain, E. B. Lobkovsky, G. W. Coates, *J. Am. Chem. Soc.* **2001**, *123*, 8738−8749; (b) D. R. Moore, M. Cheng, E. B. Lobkovsky, G. W. Coates, *Angew. Chem., Int. Ed*. **2002**, *41*, 2599−2602; (c) B. Y. Lee, , H. Y. Kwon, S. Y. Lee, S. J. Na, S. I. Han, H. Yun, H. Lee, Y.-W. Park, *J. Am. Chem. Soc.* **2005**, *127*, 3031−3037; (d) M. Kröger, C. Folli, O. Walter, M. Döring, *Adv. Synth. Catal*. **2005**, *347*,

1325−1328; (e) M. R. Kember, P. D. Knight, P. T. R. Reung, C. K. Williams, *Angew. Chem., Int. Ed.* **2009**, *48*, 931−933.

[15] M. Alvaro, C. Baleizao, E. Carbonell, M. El Ghoul, H. Garcia, B. Gigante, *Tetrahedron*, **2005**, *61*, 12131–12139.

[16] (a) X. B. Lu, X. J. Feng, R. He, *Appl. Catal., A* **2002**, *234*, 25−33; (b) B. Liang, Y. J. Zhang, Y. Z. Tian, Y. M. Wang, C. X. Bai, H. Wang, R. Zhang, J. *Am. Chem. Soc*. **2004**, *126*, 3732−3733; (c) D. J. Darensbourg, D. R. Billodeaux, *Inorg. Chem*. **2005**, *44*, 1433−1442; (d) W. Clegg, R. W. Harrington, M. North, R. Pasquale, *Chem. Eur. J.* **2010**, *16*, 6828−6843; (e) J. Meléndez, M. North, R. Pasquale, *Eur. J. Inorg. Chem.* **2007**, 3323−3326; (f) H. Sugimoto, H. Ohtsuka, S. Inoue, *J. Polym. Sci., Part A: Polym. Chem*. **2005**, *43*, 4172−4186; (g) C. Chatterjee, M. H. Chisholm, *Inorg. Chem.* **2011**, *50*, 4481−4492.

[17] S. Supasitmongkol, P. Styring *Catal. Sci. Technol*. **2014**, *4*, 1622–1630.

[18] (a) Darensbourg, D. J.; Yeung, A. D. *Polymer Chemistry* **2014**, 5, 3949-3962; (b) K. Yamaguchi, K. Ebitani, T. Yoshida, H. Yoshida, K. Kaneda, *J. Am. Chem. Soc*. **1999**, *121*, 4526-4527; (c) T. Yano, H. Matsui, T. Koiki, H. Ishiguro, H. Fujihara, M. Yoshihara, T. Maeshima, *Chem. Commun*. **1997**, 1129-1130; (d) D. J. Darensbourg, M. W. Holtcamp, *Coord. Chem. Rev*. **1996**, 153, 155 -174.

[19] (a) M. Drees, M. Cokoja, F. E. Kühn, *ChemCatChem* **2012**, *4*, 1703-1712; (b) S. Marmitt, P. F. B. Gonçalves, *J. Computat. Chem*., **2015**, *36*, 1322–1333; (c) H. Sun and D. Zhang, *J. Phys. Chem. A,* **2007**, *111*, 8036–8043; (d) J. K. Lee, Y. J. Kim, Y. S. Choi, H. Lee, J. S. Lee, J. Hong, E. K. Jeong, H. S. Kim, M. Cheong, *Appl. Catal. B*, **2012**, *111–112*, 621–627; (e) J.-Q. Wang, J. Sun, W.-G. Cheng, K. Dong, X.-P. Zhang, S.-J. Zhang, *Phys. Chem. Chem. Phys.*, **2012**, *14*, 11021–11026; (f) Y. Ren, C. H. Guo, J. F. Jia, H. S. Wu, *J. Phys. Chem. A*, **2011**, *115*, 2258–2267; (g) J. Ma, J. Liu, Z. Zhang, B. Han, *Green Chem.*, **2012**, *14*, 2410–2420; (i) M. L. Man, K. C. Lam, W. N. Sit, S. M. Ng, Z. Zhou, Z. Lin, C. P. Lau, *Chem. Eur. J*., **2006**, *12*, 1004–1015; (j) C.-H. Guo, J.-Y. Song, J.-F. Jia, X.-M. Zhang, H.-S. Wu, *Organometallics*, **2009**, *29*, 2069–2079; (k) C. H. Guo, X. M. Zhang, J. F. Jia, H. S. Wu, *J. Mol. Struct.: THEOCHEM*, **2009**, *916*, 125–134; (l) C. H. Guo, H. S. Wu, X. M. Zhang, J. Y. Song, X. Zhang, *J. Phys. Chem. A*, **2009**, *113*, 6710–6723; (m) F. Castro-Gómez, G. Salassa, A. W. Kleij, C. Bo, *Chem. Eur. J.*, **2013**, *19*, 6289–6298; (n) M. J. Ajitha and C. H. Suresh, *Tetrahedron Lett.*, **2011**, *52*, 5403–5406; (n) S. Foltran, R. Mereau, T. Tassaing, *Catal. Sci. Technol*. **2014**, *4*, 1585-1597; (o) H. Sun, D. Zhang, *J. Phys. Chem A* **2007**,*111*, 8036-8043.

[20] M. North, *Chemistry Today* **2012,** *30* May/June.

[21] A. D. Becke, *J. Chem. Phys*. **1993**, *98*, 5648–5652.

[22] P. J. Stephens, F. J. Devlin, C. F. Chabalowski, M. J. Frisch, *J. Phys. Chem*. **1994**, *98*, 11623–11627.

[23] K. Fukui, *J. Phys. Chem.* **1970**, *74*, 4161–4163.

[24] Gonzalez, C.; Schlegel, H. B. *J. Chem. Phys*. **1989**, 90, 2154–2161.

[25] Gaussian 09, Revision **D.01**, M. J. Frisch, G. W. Trucks, H. B. Schlegel, G. E. Scuseria, M. A. Robb, J. R. Cheeseman, G. Scalmani, V. Barone, B. Mennucci, G. A. Petersson, H. Nakatsuji, M. Caricato, X. Li, H. P. Hratchian, A. F. Izmaylov, J. Bloino, G. Zheng, J. L. Sonnenberg, M. Hada, M. Ehara, K. Toyota, R. Fukuda, J. Hasegawa, M. Ishida, T. Nakajima, Y. Honda, O. Kitao, H. Nakai, T. Vreven, J. A. Montgomery, Jr., J. E. Peralta, F. Ogliaro, M. Bearpark, J. J. Heyd, E. Brothers, K. N. Kudin, V. N. Staroverov, R. Kobayashi, J. Normand, K. Raghavachari, A. Rendell, J. C. Burant, S. S. Iyengar, J. Tomasi, M. Cossi, N. Rega, J. M. Millam, M. Klene, J. E. Knox, J. B. Cross, V. Bakken, C. Adamo, J. Jaramillo, R. Gomperts, R. E. Stratmann, O. Yazyev, A. J. Austin, R. Cammi, C. Pomelli, J. W. Ochterski, R. L. Martin, K. Morokuma, V. G. Zakrzewski, G. A. Voth, P. Salvador, J. J. Dannenberg, S. Dapprich, A. D. Daniels, Ö. Farkas, J. B. Foresman, J. V. Ortiz, J. Cioslowski, and D. J. Fox, Gaussian, Inc., Wallingford CT, 2009.

[26] G. Scalmani M. J.Frisch, *J. Chem. Phys.* **2010**, *132*, 114110-114112.

[27] D. A. McQuarrie, J. D. Simon, *Molecular thermodynamics*; University Science Books: Sausalito, CA, **1999**.

[28] D.H. Wertz, *J. Am. Chem. Soc*. **1980**, *102*, 5316-5322.

[29] (a) J. P. Foster, F. Weinhold*, J. Am. Chem. Soc*., **1980**, *102*, 7211-7218. (b) A. E. Reed, R. B. Weinstock, F. Weinhold, *J. Chem. Phys.* **1985,** *83*, 735-46. (c) A. E. Reed, F. Weinhold, *J. Chem. Phys*., **1985**, *83*, 1736-40. (d) J. E. Carpenter, F. Weinhold, *J. Mol. Struct. (Theochem)*, **1988**, *46*, 41-62. (e) A. E. Reed, L. A. Curtiss, F. Weinhold, *Chem. Rev*. **1988**, *88*, 899-926. (f) F. Weinhold, J. E. Carpenter, *In The Structure of Small Molecules and Ions*, Ed. R. Naaman, Z. Vager (Plenum), **1988**, 227-36.

Entry for the Table of Contents

FULL PAPER

DFT was used to investigate the cycloaddition reaction of CO_2 to styrene oxide for the formation of styrene carbonate. The uncatalyzed process alongside the reactions assisted by tetrabutylammonium bromide (**TBAB**), the novel non-symmetrical single-centre aluminium(III) salen-acac hybrid complex (salenac) (**Al1cat**) and the binary **Al1cat/TBAB** system were all investigated and for all of them lowest energy barrier reaction pathways were intercepted for both gas-phase and solvent environments.

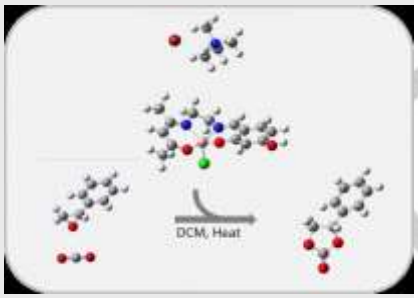

*Valeria Butera, Nino Russo, Ugo Cosentino, Claudio Greco, Giorgio Moro, Demetrio Pitea and Emilia Sicilia**

Page No. – Page No.

Computational insight on CO_2 fixation to produce styrene carbonate assisted by a single centre Al(III) catalyst and quaternary ammonium salts